Microwave stimulated combustion investigated by laser diagnostics and chemical kinetics

A. Ehn[*, 1], T. Hurtig[2], P. Petersson[1], N. Zettervall[2], B. Zhou[1], J. Zhu[1], Z.S. Li[1], M. Aldén[1], C. Fureby[2], A. Larsson[2], J. Larfeldt [3]

[1]Division of Combustion Physics, Lund University, Sweden
[2] Defence & Security Systems and Technology, Swedish Defence Research Agency – FOI, Sweden
[3]Siemens Industrial Turbomachinery AB, Finspång, Sweden

Abstract
Microwave stimulated turbulent combustion has been experimentally and computationally examined in a low-swirl burner configuration. Experimental work has focused on laser-induced fluorescence of formaldehyde (CH_2O) and methylidyne radicals (CH) as well as studies of flame emission. A reduced 102 step chemical kinetics model has been developed with the aim of implementation in combustion Large Eddy simulations. The experimental and simulated results show consistent trends with obvious increase in flame speed which result in better flame stability when a microwave field is applied to stimulate the flame.

Introduction

Research on Plasma-assisted combustion has attracted an increasing interest the last decade due to the potential of combustion enhancement and control [1]. Such features would imply combustion at lower flame temperatures as well as restraining growth of combustion instabilities to reduce NO_x-formation and emission of unburned hydrocarbons, respectively. One option is to add electric energy in the form of microwave radiation to the combustion process. The intent is that the microwave radiation is absorbed by the flame without formation of microwave-breakdown discharge. Previous investigations assert that microwave stimulation of laminar flames have shown an increase in laminar flame speed without occurrence of microwave discharges [2]. Rao et al. saw similar effects at lower electric fields as well as an increase in occurrence of excited hydroxyl radicals (OH) and carbon monoxide (CO) in a laminar flame [3]. Further, as they increased the input power of microwaves a plasma plume was formed in the flame region which affected the flame structure and significantly lowered the flammability limit.

Yu et al. investigated chemical kinetic modeling of the influence of microwave interaction with a methane-air flame using a modified version of the GRI1.2 mechanism [4]. The electron number density obtained was in good agreement with previous experimental results [5]. Furthermore, sensitivity analysis revealed that the electron number density is dominated by the chemionization reaction $CH+O->HCO^+ + e$ and that excited CH* plays a negligible role in electron formation.

The long term goal of the present work is to make energy conversion in gas turbines more efficient. The studies are similar to what was conducted by Rao et al. but instead using a 30 kW turbulent low-swirl flame that is run with lean methane/air gas mixtures. Initial experimental tests have shown increasing flame activity together with an increased occurrence of flame luminescence with increasing microwave power. In addition, the increased activity of the flame seems to allow it to burn at leaner flame conditions. Planar laser-induced fluorescence of CH_2O and CH have been conducted for pinpointing effects of the microwave stimulation in the preheat and reaction zone, respectively. Reduced kinetics mechanisms have being developed for Combustion Large-Eddy simulations to model microwave-assisted combustion in the low-swirl geometry. Here, results from a newly developed reduced mechanism are presented. The mechanism is based on a reduced methane/air mechanism where reduced submechanisms of ozone and singlet oxygen chemistry, chemiionization and electron impact as well as excited states of nitrogen are included.

Experimental Setup

Low swirl burner

For investigating the influence of microwave stimulation a lean premixed lifted flame stabilized by a low-swirl burner was used [6, 7]. The low-swirl flow is created by an outer annular swirler, with eight swirl-vanes, in combination with an inner perforated plate that allows for about 40% by volume of the mixture to pass through (Figure 1) [7]. After passing the swirler/perforated plate premixed methane/air discharges through a 50 mm nozzle into a cylindrical

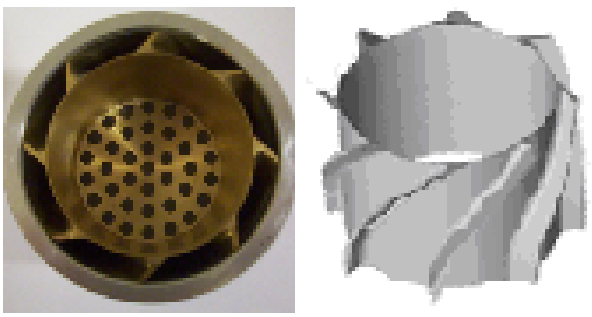

Figure 1 The annular swirler and the inner perforated plate.

[*] Corresponding author: andreas.ehn@forbrf.lth.se

chamber (300 mm in diameter) with a co- flow of air of 0.4 m/s. The chamber in combination with two metallic meshes is used as an enclosure for the applied microwave field, see below Figure 3a. To assure well-controlled experimental conditions the set-up includes calibrated mass flow controllers for methane and air (Bronckhorst Hi-Tec, EL-Flow), and a flow meter for the co-flow (Fox, Thermal Instruments).

The resulting outflow from the nozzle has an inner low velocity non-swirling region (-10 mm< r < 10 mm, r = radius) and an outer region with higher axial and tangential velocities [6, 7]. Away from the nozzle the flow diverges causing the axial velocity in the center region to gradually decrease to create a low-speed region where the freely propagating turbulent flame can be stabilized. The investigated flames are categorized in the flamelet (leading edge) and the thin reaction zone regime (trailing edge) of the turbulent combustion diagram [8]. In previous studies of lean unconfined methane/air flames (equivalence ratio ϕ=0.62) the mean flame position at the centerline is 33 mm above the nozzle for Re=20,000, and slightly lower for Re=30,000 [7]. With the present set-up the flow field is expected to be moderately influenced by the mesh above the nozzle exit compared to previously performed studies. However, as only relative changes, with and without microwave stimulation, of the mean flame position and shape are of interest in this investigation the influence of the mesh on the flow field can be accepted.

Microwave system

The microwave system consist of a National Electronics GA15MP, 2.45 GHz, industrial magnetron including a circulator and a load to absorb reflected power, sensors for incident and reflected power and a three stub tuner, see Figure 2. The magnetron is capable of delivering up to 15 kW of microwave power into a matched load. However, in the experiments reported here the maximum power absorbed by the flame never exceeds

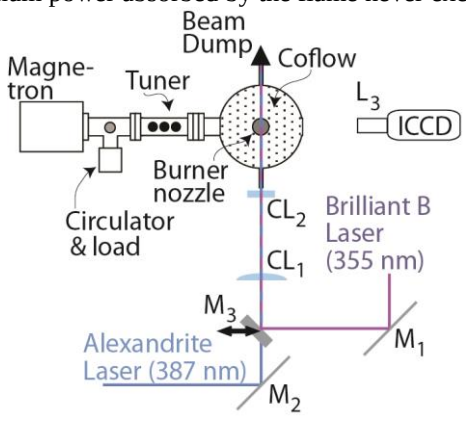

Figure 2 Schematic picture of microwave setup and the coupling of microwaves via the tuner into the resonant chamber and the flame. The 355 nm laser beam is directed into the optical path of the 387 nm beam using a kinematic mirror (M_3). Two Cylinder lenses (CL) are used to create a laser sheet and an ICCD camera acquires PLIF images through the view port which is equipped with a double mesh.

300 W, which is about 1% of the total effect of the flame. Incident and reflected microwave power is measured by means of Herotek DZM124AB microwave diodes coupled to electric field sensors built into the circulator.

The aluminum chamber has two slits and together with a view port in the chamber PLIF measurements are possible to carry out. Leakage of microwave radiation from the slits into the surrounding lab is avoided by making the slits narrow and by mounting microwave traps, i.e. metallic tubes that do not allow for radiation of the wavelength used to escape. The view port is shielded by the use of a metallic mesh. In order to create a simple resonant cavity around the flame two metallic meshes are used, one just above the burner nozzle (but below the actual flame) and one at the top of the cavity, see Figure 2. The microwave chamber around the burner is designed to resonate in the TM026 mode at 2.45 GHz, see Figure 3a. The mode pattern was modeled and experimentally investigated at the bottom of the chamber using temperature sensitive liquid crystal sheets (Edmund Optics). These experimental results are in good agreement to the simulated results that are displayed in Figure 3b.

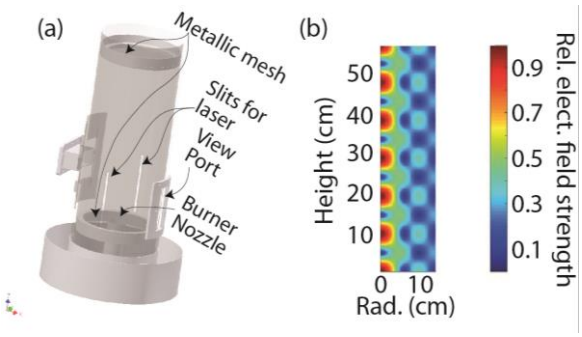

Figure 3 (a) CAD representation of the burner and the microwave cavity. Two metallic meshes are used to create a cylindrical cavity in, and around, the flame region. The cavity is designed to resonate at the TM026 mode. (b) Representation of the relative field strength for the TM026 mode inside the microwave cavity.

Optical arrangement

Two separate laser systems were used to study the spatial distribution of CH and CH_2O which are distributed in the reaction zone and the preheat zone, respectively. An Alexandrite laser (101PAL, Light Age), tuned to 387 nm, was used for excitation of CH, where a detailed description of the excitation scheme is given by Li et al. [9]. Formaldehyde was probed by a frequency tripled Brilliant B laser (Quantell) providing 355 nm laser pulses with a pulse duration of less than 10 ns. The optical arrangement is displayed in Figure 2. The molecular distributions were sequentially measured using a kinematic mount for the M_3 mirror to alternate between the excitation schemes. The laser beams are entering the aluminum microwave cavity through a 50 mm long aluminum tube with an inner diameter of 20 mm. This microwave-trap arrangement allows the laser

beams to enter the measurement volume while it prevents microwave to leak out. The laser beams are focused in the center of the low swirl flame using a quartz cylinder lens (CL_1) with a focal length of 1000 mm. A negative quartz cylinder lens (CL_2), with a focal length of -40 mm, was used to expand the beams in the vertical direction to form a slightly diverging laser sheet with an approximate height of 5 cm in the measurement volume. This type of diverging arrangement was arranged in order to form a large-enough laser sheet through the microwave trap. A built-in metal beam dump was used to dump the laser light in the chamber which was spray painted with graphite to minimize scattered laser light.

A PI-MAX 3 ICCD camera (Princeton Instruments) was used to capture PLIF data. The camera was equipped with a 50 mm/1.2 Nikon lens where double GG400 Schott filters (1 mm thick) were used to discriminate stray laser light.

Modeling System

Simulations were carried out using Cantera [10]. The base of the kinetic mechanism used is a 42-step skeletal methane-air mechanism consisting of 18 species, here called Z42. This mechanism is well characterized both for a wide range of equivalence ratios but also for different temperatures and pressures. Added to that skeletal mechanism is a series of sub mechanisms starting with a thirteen step ozone reaction sub mechanism and an eight step singlet oxygen sub mechanism. Reactions for chemiionization, electronic excitation, electron impact dissociation, electron impact ionization, electron impact and excited nitrogen states are also added which all in all gives a skeletal mechanism consisting of 102 reactions and 31 species. The reaction rates for these reactions were taken from Aleksandrov et al. and Prager et al. [11, 12] and calculated from electron cross sections using the free software BOLSIG+ [13].

Results and Discussion

The experiments presented in this paper were conducted at varying equivalence ratio ranging from 0.57 to 0.62. With an inlet gas temperature of 300 K and pressure of 1 atm the laminar flame speed, at ϕ = 0.62, calculated using Peters' mechanism [14] is 12 cm/s. The Reynolds numbers (Re) based on the bulk flow velocity of 6.2 m/s and diameter at the burner exit were about 20 000.

Flame emission

The ICCD camera was used to acquire flame emission at different electric field strengths. Thirty images, each with an acquisition time of 1 s, are averaged for good statistics of the turbulent flame. In these measurements ϕ was 0.57 and measurements were conducted both with and without microwave stimulation. The absorbed microwave power was roughly 100W. Averaged images of the flame emission with and without microwave stimulation are shown in Figure 4a and b, respectively.

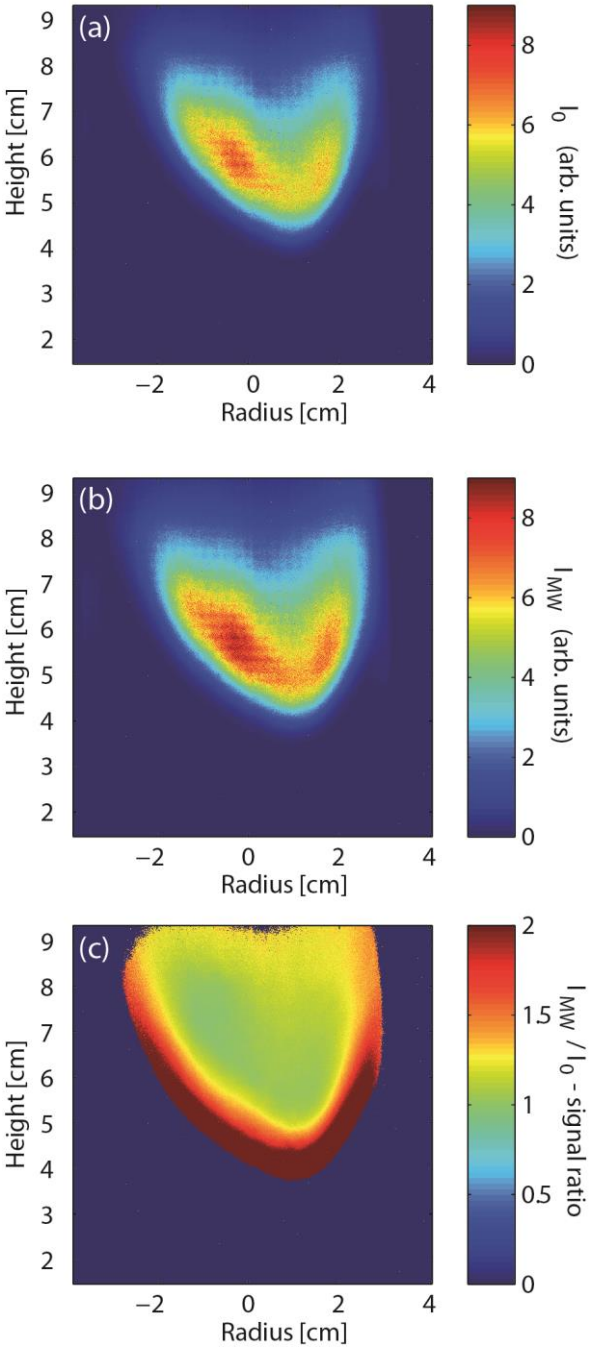

Figure 4 Averaged flame emission data (a) without microwave stimulation and (b) with microwave stimulation. (c) Images in (a) and (b) are arranged in a ratio to visualize the changes in signal with respect to microwave stimulation.

Identical colorbars are used to visualize the two images and it is obvious that the signal intensity is increased with microwave stimulation. A ratio of the two images is displayed in Figure 4c indicating a signal increase of 10-15% in the area where the strongest signal is seen. The signal in the nominator of the ratio (I_{MW}) is cut off using a threshold signal intensity of about 5% of its maximum in order to suppress the noise that appears at locations where the denominator signal is

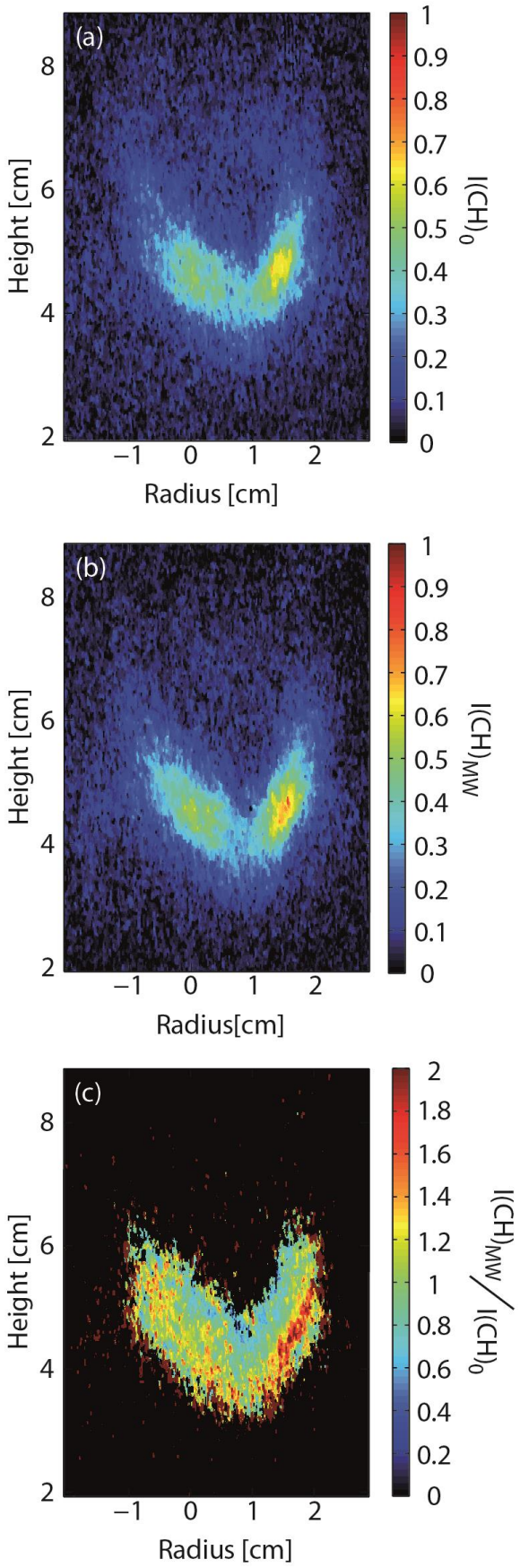

Figure 5 Averaged CH PLIF images (a) without and (b) with microwaves. (c) A ratio image of (b)/(a).

close to zero. In addition, the difference in signal strength increases further down towards the nozzle.
The most obvious reason for this difference in signal distributions is that the flame moves towards the burner when microwaves are interacting with the flame. However, flame emission is acquired in line of sight and since the flame diameter is smaller at the bottom the intensity difference is enhanced at lower positions in the flame.

Laser induced fluorescence of CH

Planar laser-induced fluorescence of CH was performed and averaged distributions of CH are displayed in Figure 5a and b without and with microwaves, respectively. Imaging of CH PLIF is frequently used as a flame front marker and are therefore of interest in terms of the energy coupling of electric power to the flame chemistry. The averaged data, shown in Figure 5a and b consists of 300 single-shot images that have been corrected for background. Furthermore, a median filter has been used to get rid of erroneous pixel values and strong scattering. By comparing Figure 5a and b, it seems like the flame is shifted a little bit to the right and that the CH-PLIF signal is slightly increased. This signal increase might be a result of more stable combustion with microwave stimulation and that the CH-distribution therefore is confined in a smaller volume. Further, even though the signal is somewhat noisy Figure 5c indicates that the signal is shifted downwards when the flame is exposed to microwaves since the upper part of the signal ratio is below 1 and the lower part has a reddish tone indicating a value above 1.

Laser induced fluorescence of CH_2O

Formaldehyde is a product in the early stages of combustion that occur below and around 1000 K [15]. Previous work has shown that ozone, which is a typical plasma product, has an effect on the initial phase of combustion [16, 17]. Formaldehyde concentration is increased when ozone is added to premixed methane/air flames as a result of excessive increase in O-atom concentration. Formaldehyde PLIF images captured from measurements with and without microwave stimulation are shown in Figure 6a and b, respectively. These images show averaged data from 300 single-shot images that has been corrected for background. The images show a substantial difference due to the effect of microwave stimulated combustion. First, there is a clear indication that the formaldehyde distribution is shifted closer to the burner nozzle. This is a result similar to what was reported by Ehn et al. [16] when ozone was seeded into the flame, which shows that the applied microwave field enhances the flame speed. Second, there is a substantial formaldehyde signal in the top of the image, about 8 cm above the burner nozzle. This signal increase when ϕ is reduced and the flame gets less stable. Previous results, presented by Carlsson et al. have shown that unburned hydrocarbons recirculate into the center of the flame further downstream [18]. In addition Zhou and co-workers showed that a second

regime of combustion occurs downstream as the recirculated fuel is consumed [19]. These results show

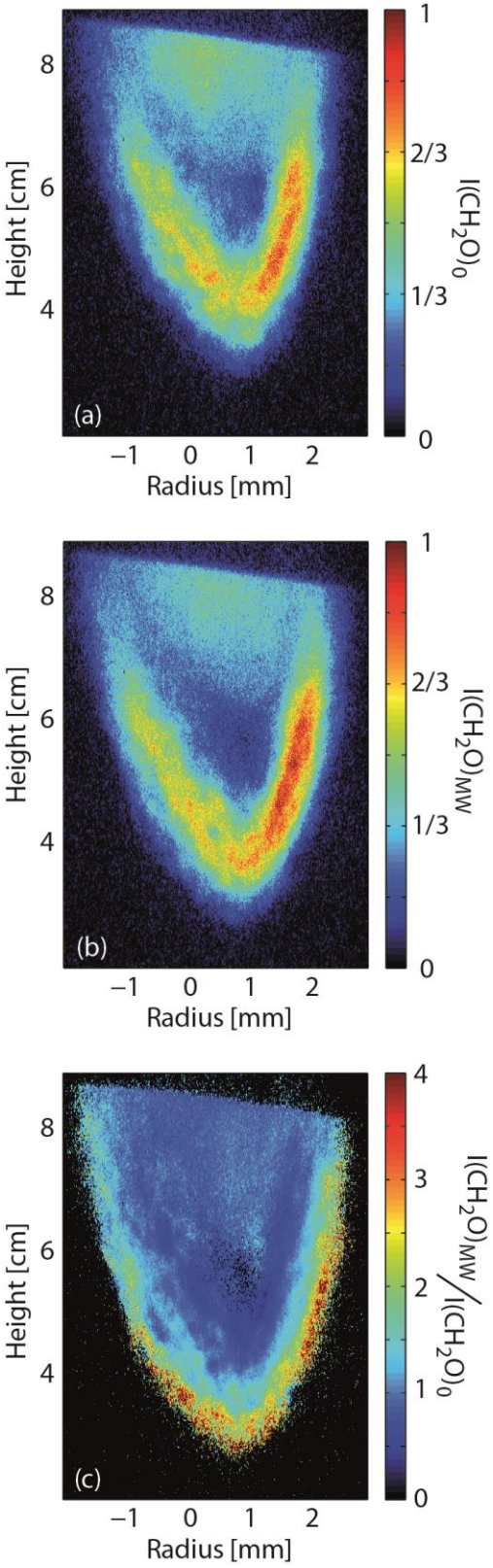

Figure 6 Planar laser-induced fluorescence of CH_2O are shown (a) without applying microwaves to the flame and (b) with microwaves. (c) A Ratio of the images (b) and (a) is shown to illustrates the effect of microwave stimulation of the flame.

that the formaldehyde signal, that is located downstream, is decreased as microwaves are present in the measurement volume. Altogether, these results indicate that the applied microwave field seems to make the flame more stable and therefore lower losses of unburned hydrocarbon in the emission.

Third, the formaldehyde signal strength, stemming from the formaldehyde that is produced in the near vicinity of the leading edge, is increased as the flame is stimulated by a microwave field. The flame shift and signal enhancement that is seen upstream is better illustrated in Figure 6c where a ratio of the two images from Figure 6b and Figure 6a are displayed. Note that the color bar is adjusted to show the range 0 to 4, where the center of the flame displays a value around 1 or lower.

Chemical kinetics

Laminar flame speed vs ϕ calculated using the newly developed reduced kinetic mechanism for three different values of reduced electric field strength, 0 Td, 50 Td and 100 Td, can be seen in Figure 7. Here Td stands for Townsend and is the unit used to denote the reduced electric field, 1 Td = 10^{21} * E/N [Vm^2], where E is the electric field in V/m and N is the gas number density given in m^{-3}.

The blue, red and green curves show results that were calculated using the newly developed 102-step reaction mechanism. Results that serve as a reference are show in black and these simulations were carried out without applying any electric field using the well-established GRI 3.0 mechanism [20]. The results from the reference simulation agree fairly well with the green curve, indicating that the reduced 42 step methane combustion mechanism provides fairly accurate flame speeds. Obviously the flame speed increases with increased field strength of the electric field, which resonates well with the experimental results that are presented above.

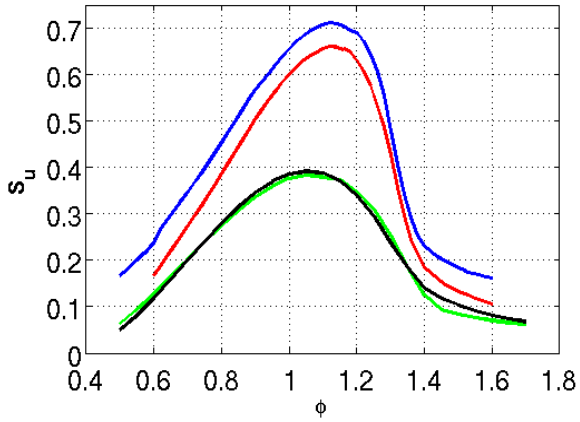

Figure 7 Laminar flame speed vs phi calculated using the newly developed reduced kinetic mechanism for three reduced electric field strengths. The green, red and blue curves represent data for 0, 50 and 100 Td, respectively. The black curve represents reference data that is calculated without any electric field using the GRI3.0 mechanism.

Conclusion

A turbulent 30 kW low-swirl flame is investigated as it is being stimulated by an external electric microwave field. The microwave stimulation increases the chemiluminescence as well as the PLIF signal from CH and CH_2O. This increase in signal intensities is accompanied by a shift of the distributions of these signals which are moved closer to the burner nozzle indicating an increase in flame speed for the turbulent flame as microwaves are applied to the flame. This is supported by CANTERA simulations where a newly developed reduced chemical kinetics model predicts similar trends. The reduced kinetic model is based on 102 reactions were of which 42 reactions describes the methane/air chemistry, ozone and singlet chemistry are described by 13 and eight reaction steps, respectively, whereas chemiionization, electronic excitation, -impact dissociation, -impact ionization, -impact and excited nitrogen states are described by the residual ones. This work is ongoing with the next step of quantifying the experimental conditions and using these conditions as input values in combustion LES simulations where the reduced chemistry is implemented.

Acknowledgements

This work was financed by the Swedish Energy Agency via the project number 36646-1 as well as the EFFECT and the CECOST projects. Further, Knut & Alice Wallenberg Foundation, and European Research Council also contributed with funding for this work. Finally, J. Zhu would like to thank China Scholarship Council for financial support.

References

[1] A. Starikovskiy, N. Aleksandrov, Prog. Energy Combust. Sci., 39 (2013) 61-110.

[2] E.S. Stockman, S.H. Zaidi, R.B. Miles, C.D. Carter, M.D. Ryan Combust. Flame 156 (2009) 1453-1461.

[3] X. Rao, K. Hemawan, I. Wichman, C. Carter, T. Grotjohn, J. Asmussen and T. Lee, Proc. Comb. Inst. 33 (2011) 3233-3240.

[4] Y. Ju, S.O. Macheret, M.N. Shneider and R.B. Miles, 40th AIAA Joint propulsion Conference & Exhibit, Fort Lauderdale, Florida, 11.-14 July, 2004, AIAA 2004-3707.

[5] C.S. MacLatchy, Combust. Flame 36 (1979) 171-178.

[6] K.J. Nogenmyr, P. Petersson, X.S. Bai, A. Nauert, J. Olofsson, C. Brackman, H. Seyfried, J. Zetterberg, Z.S. Li, M. Richter, A. Dreizler, M. Linne, and M. Alden, Proceedings of the Combustion Institute, 2007. 31: p. 1467-1475.

[7] P. Petersson, J. Olofsson, C. Brackman, H. Seyfried, J. Zetterberg, M. Richter, M. Alden, M.A. Linne, R.K. Cheng, A. Nauert, D. Geyer, and A. Dreizler, Applied Optics, 2007. 46(19): p. 3928-3936.

[8] N. Peters, Turbulent combustion, 2000: Cambridge University Press. xvi, 304 p.

[9] Z.S. Li, J. Kiefer, J. Zetterberg, et al. Proc. Combust. Inst., 31 (2007), pp. 727–735.

[10] Cantera Developers (2012). Cantera: Chemical kinetics, Thermodynamics, Transport properties. [Online]. Available: http://cantera.github.com/docs/sphinx/html/index.html.

[11] N.L. Aleksandrov. S. V. Kindysheva, E.N. Kukaev, S.M. Starikovskaya, and A.Yu. Starikovskii, Plasma Physics Reports, 2009, Vol. 35, No. 10, pp. 867–882.

[12] J. Prager, U. Riedel, J. Warnatz, Proceedings of the Combustion Institute 31 (2007) 1129–1137.

[13] G. J. M. Hagelaar and L. C. Pitchford, Plasma Sources Sci. Techn. 14 (2005) 722-733.

[14] N. Peters and B. Rogg, Reduced kinetic mechanisms for applications in combustion systems. Lecture notes in physics New series m, Monographs1993, Berlin ; New York: Springer-Verlag. x, 360 p.

[15] J. F. Griffiths and J. A. Barnard, Flame and Combustion, 3rd edition, Chapman and Hall, London, UK, 1995.idge University Press. xvi, 304 p.

[16] A Ehn, J. Zhu, P. Petersson, Z-S Li, M. Alden, C. Fureby, et al. Proc Combust Inst; Volume 35, Issue 3, 2015, 3487–3495.

[17] W. Weng, E. Nilsson, A. Ehn, J. Zhu, Y. Zhou, Z. Wang, Z-S Li, M. Aldén, K. Cen, in press in Combustion and flame 2015, doi:10.1016/j.combustflame.2014.10.021.

[18] H. Carlsson, E. Nordström, A. Bohlin, P. Petersson, Y. Wu, R. Collin, M. Aldén, P-E Bengtsson, X-S Bai, Combust. Flame Vol. 161, Issue 10, Pages 2539–2551.

[19] B. Zhou, Q. Li, Y. He, P. Petersson, Z-S Li, M. Aldén, X-S Bai, Submitted to Combust. Flame, Oct 2014.

[20] F. Frenklach, H. Wang, C. L. Yu, M. Goldenberg, C. T. Bowman, R. K. Hanson, D. F. Davidson, E. J. Chang, G. P. Smith, D. M. Golden,W. C. Gardiner and V. Lissianski: http://www.me.berkeley.edu/gri_mech.